JOURNAL OF THEORETICAL AND APPLIED MECHANICS
51, 3, pp. 729-739, Warsaw 2013

LATTICE BOLTZMANN SIMULATION OF NATURAL CONVECTION FLOW AROUND A HORIZONTAL CYLINDER LOCATED BENEATH AN INSULATION PLATE

Abbasali Abouei Mehrizi
Young Researchers Club, Karaj Branch, Islamic Azad University, Karaj, Iran
e-mail: abbasabouei@gmail.com; a.abouei@stu.nit.ac.ir

Mousa Farhadi, Hamid Hassanzadeh Afrouzi
Department of Mechanical Engineering, Babol University of Technology, Babol, Iran

Saeed Shayamehr
ATEC Engineering Consultants, Tehran, Iran

Hossein Lotfizadeh
Islamic Azad University, Karaj Branch, Karaj, Iran

In this paper, two-dimensional heat transfer solution of natural convection around an isothermal cylinder located beneath an insulation wall is studied. The effects of distance ratio of the cylinder to the wall as well as the impact of the dimensionless Rayleigh number in the flow and heat transfer are taken into account. Solving the flow equations for L/D ratio with values 0.5, 0.7, and 1.5 and the Rayleigh number ranging from 1000 to 40000 is carried out. The results are compared with the experimental data which present a good agreement. The results indicate that the effect of weakened natural convection flow in the cylinder commences when decreasing L/D ratio from the value 1.5 to 0.5 leading to a decline in heat transfer and the Nusselt number. This process occurs in all values of the Rayleigh number. For the ratio number greater than 1.5, the impact of adiabatic wall is neglected, and there is no significant influence on the natural convection flow. Increasing the angle from 0°to180°results in a fall in the Nusselt number which is as a consequence of growth in the distances of isothermal lines.

Key words: free convection, isothermal cylinder, Lattice Boltzmann Method (LBM)

Nomenclature

c – discrete lattice velocity
D – diameter of cylinder
F – external force
f, g – distribution function for density and temperature, respectively
g_y – gravity acceleration in y direction
L – distance between cylinder and adiabatic wall
Nu, Ra – Nusselt and Rayleigh $(\mathrm{Ra} = g\beta\Delta T D^3/(\alpha\nu))$ number, respectively
$t, \Delta t$ – time and lattice time step, respectively
$T = (\Theta - \Theta_\infty)/(\Theta_c - \Theta_\infty)$ – non-dimensional temperature
$W = 20D$ – width of insulation wall
w – weighing factor
$\mathbf{x} = (x\mathbf{i} + y\mathbf{j}), \mathbf{u} = (u\mathbf{i} + v\mathbf{j})$ – location and velocity vector, respectively
β – thermal expansion coefficient
$\delta = |x_f - x_w|/|x_f - x_b|$ – fraction of intersected link in fluid region

θ – angle from stagnation
Θ – temperature
ν – kinematic viscosity
ρ – density
τ_t, τ_v – relaxation time for temperature and velocity equation, respectively
χ – weighing factor

Subscripts: avg – average, b – boundary nodes, c – cylinder, f, ff – first and second fluid nodes, respectively, i – lattice model direction, L – local, s – sound, ∞ – ambient condition.
Superscripts: eq, neq – equilibrium and non-equilibrium distribution function, respectively.

1. Introduction

In general, natural convection heat transfer occurs as a result of temperature difference between the fluid and the solid boundary. The temperature gradient leads to creation of a non-uniform density field. But, it is in fact a body force dependent on the density causing the fluid to move. This force is the gravitational force. As a whole, because of various functions of the heat transfer around a cylinder, the issue is highly prominent to the scientists and there have already been a lot of studies conducted on this subject. Morgan (1975) reviewed more than 250 scientific articles about the natural convection around an individual cylinder in a review paper. Numerical solution of Qureshi and Ahmad (1989) and benchmark solution of Saitoh *et al.* (1993) are known to be among the most authentic solutions. Heat transfer around a horizontal cylinder close to the wall or surrounded by walls has been studied thoroughly by a lot of researchers. Marsters (1975) studied the effect of the existence of the wall near the horizontal cylinder for the Rayleigh number ranging from 10 to 500000 and presented a correlation among Nusselt distribution, Rayleigh number and geometric parameters. Sadeghipoor and Razi (2001) developed a code using the finite element method to simulate the two-dimensional transient convective flow in a laminar regime. They also studied heat transfer from a horizontal cylinder surrounded by two insulation walls. The results show good agreement with the experimental data. Moreover, the optimum wall distance from the cylinder, in order to reach the maximum value of the Nusselt number, was achieved in the study. Natural convection heat transfer around a horizontal cylinder located between two walls was studied by Ma *et al.* (1994). The effect of vertical displacement of the cylinder was also taken into consideration in this study. Convection heat transfer on a horizontal cylinder laid under a flat plate has a lot of applications including heat transfer around pipes carrying hot fluid, electronic industry and heat transfer in the cylindrical components assembled under electronic boards. Koizumi and Hosokawa (1996) utilized a flow detector to draw the flow regime around an isothermal cylinder located under an adiabatic wall. The experiment was conducted using air as the working fluid for the Rayleigh number ranging from $4.8 \cdot 10^4$ to $1 \cdot 10^7$. It was concluded that the patterns of streamlines and temperature counter are dependent on the Rayleigh number and the ratio of the plate length to the cylinder diameter. It was also proved that for small values of the Rayleigh number ($\mathrm{Ra} \leqslant 10^5$), the two-dimensional steady flow is observed for all the values of L/D. For average and high Rayleigh numbers, a three-dimensional flow is created for small values of L/D. Also, a plume which oscillates from side to side is observed above the cylinder. Meanwhile, a new method has recently been developed, named the Lattice Boltzmann Method that has been vastly successful in simulation of heat transfer and fluid flow (Shan and Chen, 1993; Fattahi *et al.*, 2010; Mehrizi *et al.*, 2012, 2013). Dixit and Babu (2006) simulated natural convection in a cavity for high values of the Rayleigh number using the Lattice Boltzmann method. And the results closely correspond to the previous experimental studies. Mohammad and Kuzim (2010) investigated mainly three different schemes of adding a force term to LBM with the BGK method. They added a term of the buoyancy external

force to the Lattice Boltzmann Method and studied natural convection in an enclosure. In addition, Mohammad and *et al.* (2009) studied natural convection in an open cavity and tested the capability of Lattice Boltzmann method in simulation of natural convection. A number of researchers have already taken into consideration the natural convection around a heated cylinder in an enclosure as well. Simulation of natural convection in the space between the internal circular cylinder and an external square enclosure was done by Peng *et al.* (2003), using Taylor series expansion and least-squares-based Lattice Boltzmann method. Jami *et al.* (2007) utilized the Lattice Boltzmann Method to simulate natural convection in a differentially heated, square enclosure with a heated cylinder at its center. The difference between their work and previous studies is heat generation in the inner conducting cylinder. Jami *et al.* (2008) considered the impact of internal cylinder displacement on the heat transfer in a separate study.

In this paper, the simulation of natural convection around a horizontal cylinder located under an insulation wall is carried out using the Lattice Boltzmann Method. The effect of the Rayleigh number between 1000 and 40000 and L/D ratio (the distance from the cylinder to the insulation wall divided by cylinder diameter) ranging from 0.5 to 1.5 is also taken into consideration. The results are compared with the experimental results achieved by Ashjaee *et al.* (2007) and also illustrated as streamlines, average values as well as local values of the Nusselt number and isotherms.

2. Geometry description and boundary conditions

As shown in Fig. 1, the geometry is an isothermal cylinder with a diameter as long as D which is located under a wide insulation plate. The distance from the cylinder to the plate is L and the insulation wall length is W. The temperature of the cylinder wall is taken constant Θ_c and the wall above the cylinder is assumed to be adiabatic. Air ($\mathrm{Pr} = 0.7$) with ambient temperature Θ_∞ is selected as the working fluid. Also, the inlet boundary condition is taken an open boundary and the boundary conditions at both sides are taken to be constant ambient pressure. Boundary conditions of the wall with a constant temperature, insulation wall, no-slip boundary condition and Zou and He's (1997) pressure boundary condition are thoroughly discussed in the applied Lattice Boltzmann Method for transport phenomena momentum heat and mass transfer written by Mohammad (2007).

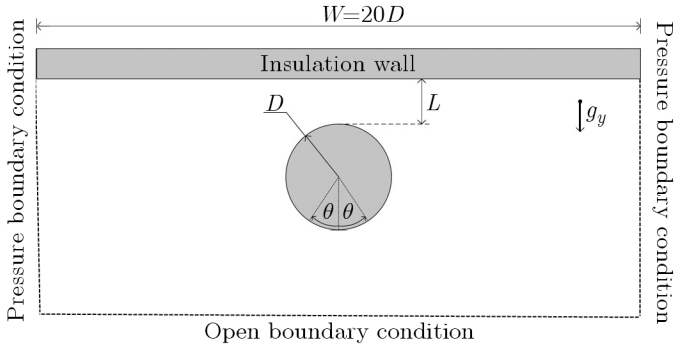

Fig. 1. Computational domain and boundary conditions

In the open boundary condition, the normal practice is to use extrapolation for the unknown distribution functions. So, at this boundary

$$f_{2,n} = 2f_{2,n-1} - f_{2,n-2} \qquad f_{5,n} = 2f_{5,n-1} - f_{5,n-2} \qquad f_{6,n} = 2f_{6,n-1} - f_{6,n-2} \tag{2.1}$$

For the adiabatic boundary condition, a second order finite difference approximation was used

$$3T_b = 4T_n - T_{n-1} - 2\Delta x \frac{\partial T}{\partial x} \tag{2.2}$$

where subscript b denotes the boundary node, subsequently n and $n-1$ denote the first and second nodes in the domain, respectively.

3. Lattice Boltzmann Method

The Lattice Boltzmann Method is one of the computational methods used to simulate fluid flow and heat transfer. This is based on the theory of kinetic energy of particles in mesoscopic scale and study of movement and collision of particles. In this method, the distribution function, which is the probability of finding particles with a certain range of velocity and place in a certain time, is replaced with studying each individual particle in the molecular dynamic simulations. In order to solve the flow and temperature fields, the values of velocity f and energy distribution functions g must be calculated in the discretized Lattice Boltzmann equation. The main equation of Boltzmann model for fluid flow with a term of an external force is expressed as follows

$$f_i(x + c_i\Delta t, t + \Delta t) = f_i(x,t) + \frac{\Delta t}{\tau_v}[f_i^{eq}(x,t) - f_i(x,t)] + \Delta t c_i F_i \tag{3.1}$$

And this equation for the temperature field is expressed as below

$$g_i(x + c_i\Delta t, t + \Delta t) = g_i(x,t) + \frac{\Delta t}{\tau_t}[g_i^{eq}(x,t) - g_i(x,t)] \tag{3.2}$$

where Δt indicates the time step, c_i represents discretized velocity of the Lattice in the direction i $(i = 0, \ldots, 8)$, F_i as the external force and finally $\tau_v = 3\nu + 0.5$ and $\tau_t = 3\alpha + 0.5$ show the lattice relaxation time for the flow and temperature field, respectively. The values of relaxation times are set to be 0.59 and 0.629 for the flow and temperature field respectively. Also in equations (2.1) and (2.2), the BGK model which was introduced by Bhatnagar, Gross and Krook (1954) is used to model the collision term in the Boltzmann equation. In the present study, the D2Q9 model with 8 directions is used for both fluid and thermal fields, and the values of weighing factor, $w_0 = 4/9$ for $|c_0| = 0$ (for the static particle), $w_{1-4} = 1/9$ for $|c_{1-4}| = 1$ and $w_{5-9} = 1/36$ for $|c_{5-9}| = \sqrt{2}$ are assigned in this model. The equilibrium distribution functions of temperature and velocity in the above equations are expressed as follows

$$f_i^{eq} = w_i\rho\Big[1 + \frac{c_i u}{c_s^2} + \frac{(c_i u)^2}{2c_s^4} - \frac{u^2}{2c_s^2}\Big] \qquad g_i^{eq} = w_i T\Big(1 + \frac{c_i u}{c_s^2}\Big) \tag{3.3}$$

The buoyancy force in the direction y, with the Boussinesq approximation applied to that, is calculated below and substituted in equation (2.1)

$$F = 3w_i g_y \beta\theta \tag{3.4}$$

Solving the equation, the values of the distribution functions f and g are defined. Using these functions, velocity, momentum, the non-dimensional temperature and macroscopic density are calculated as follows

$$\rho = \sum_k f_k \qquad \rho u_i = \sum_k f_k c_{ki} \qquad T = \sum_k g_k \tag{3.5}$$

where $T = (\Theta - \Theta_\infty)/(\Theta_c - \Theta_\infty)$ is the non-dimensional temperature.

4. Curved boundary treatment

In the present study, a second-order accuracy method is used to define the curve boundary condition (MLS boundary condition) which was developed by Mei *et al.* (1999). Figure 2 shows a part of arbitrary curved wall geometry. In this figure, the white and gray sides show the fluid and solid regions respectively. The clear white nodes in the solid region indicate the boundary nodes $\mathbf{x}_b$, the hatched nodes show the first fluid nodes $\mathbf{x}_f$, the solid gray nods show the second fluid nods $\mathbf{x}_{ff}$ and the solid block nodes on the boundary $\mathbf{x}_w$ indicates the intersections of the wall with various lattice links.

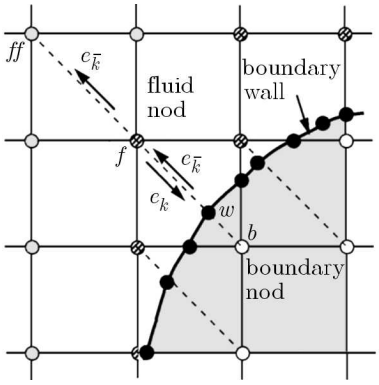

Fig. 2. Characteristics of Lattice nods and the curved wall boundary (Mei *et al.*, 1999)

The fraction of an intersected link in the fluid region δ, is determined by

$$\delta = \frac{|\mathbf{x}_f - \mathbf{x}_w|}{|\mathbf{x}_f - \mathbf{x}_b|} \tag{4.1}$$

At the collision step, the fluid side distribution function on the fluid nod $\widetilde{f}_k$ is determined but the solid side distribution function at the opposite direction $\widetilde{f}_{\overline{k}}$ is unknown. On the other hand, to finish the streaming step, we need to know $\widetilde{f}_{\overline{k}}$ at the boundary node x_b.

4.1. Velocity in the curved boundary condition

The unknown distribution function $\widetilde{f}_{\overline{k}}$ is calculated by linear interpolation that was suggested by Fillipova and Hänel (1998)

$$\widetilde{f}_{\overline{k}}(\mathbf{x}_b, t+\Delta t) = (1-\chi)\widetilde{f}_k(\mathbf{x}_f, t+\Delta t) + \chi f_k^*(\mathbf{x}_b, t+\Delta t) + 2\omega_k \rho \frac{3}{c_k^2}\mathbf{e}_{\overline{k}}\mathbf{u}_w \tag{4.2}$$

where

$$f_k^*(\mathbf{x}_b, t+\Delta t) = \omega_k \rho(\mathbf{x}_f, t+\Delta t)\Big[1 + \frac{3}{\mathbf{c}_k^2}\mathbf{e}_k\mathbf{u}_{bf} + \frac{9}{2\mathbf{c}_k^4}(\mathbf{e}_k\mathbf{u}_f)^2 - \frac{3}{2\mathbf{c}_k^2}\mathbf{u}_f\mathbf{u}_f\Big] \tag{4.3}$$

In Eq. (4.1) $\mathbf{u}_f \equiv \mathbf{u}(x_f, t+\Delta t)$ is the fluid velocity near the wall, $\mathbf{u}_{bf}$ is the imaginary velocity for interpolations, $\mathbf{e}_k$ is the unit vector in the direction of k, χ is the weighting factor which depends on $\mathbf{u}_{bf}$ and, at the MLS scheme, it is calculated as below

$$\mathbf{u}_{bf} = \begin{cases} \Big(1 - \dfrac{3}{2\delta}\Big)\mathbf{u}_f + \dfrac{3}{2\delta}\mathbf{u}_w & \text{when} \quad \delta \geqslant \dfrac{1}{2} \\ \mathbf{u}_{ff} = \mathbf{u}_f(\mathbf{x}_f + e_{\overline{k}}\Delta t, t + \Delta t) & \text{when} \quad \delta < \dfrac{1}{2} \end{cases}$$
$$\chi = \begin{cases} \dfrac{2\delta - 1}{\tau + 1/2} & \text{when} \quad \delta \geqslant \dfrac{1}{2} \\ \dfrac{2\delta - 1}{\tau - 2} & \text{when} \quad \delta < \dfrac{1}{2} \end{cases} \tag{4.4}$$

where $\mathbf{u}_{ff}$ is the velocity of the second node on the fluid side and $e_{\overline{k}} \equiv -e_k$.

4.2. Temperature in the curved boundary condition

In this study, the developed scheme of Yan and Zu (2008) is used in order to apply the curve boundary condition on the temperature field. This scheme is based on the extrapolation method with the second order accuracy. The distribution function for temperature is divided into two parts, equilibrium and non equilibrium

$$\widetilde{g}_k(x_b, t) = g_k^{eq}(x_b, t) + g_k^{neq}(x_b, t) \tag{4.5}$$

By substituting Eq. (4.4) into the temperature streaming equation $g_k(\mathbf{x} + \mathbf{c}_k\Delta t, t + \Delta t) = \widetilde{g}_k(\mathbf{x}, t + \Delta t)$, one arrives at

$$g_k(x_b, t) = g_k^{eq}(x_b, t) + \Big(1 - \frac{1}{\tau_t}\Big)g_k^{neq}(x_b, t) \tag{4.6}$$

To determine the value of $g_{\overline{k}}(x_b, t)$, values of the equilibrium and non-equilibrium parts of the distribution function should be defined. The equilibrium distribution function $g_{\overline{k}}^{eq}(x_b, t)$ can be expressed as

$$g_k^{eq}(x_b, t) = \omega_k T_b\Big(1 + \frac{3}{c^2}\mathbf{e}_k\mathbf{u}_b\Big) \tag{4.7}$$

$u_b \equiv u(x_b, t)$ and $T_b \equiv T(x_b, t)$ are the velocity and temperature on boundary nodes, respectively, and they can be approximated by

$$\mathbf{u}_b = \begin{cases} \dfrac{1}{\delta}[\mathbf{u}_w + (\delta - 1)\mathbf{u}_f] & \text{if} \quad \delta \geqslant \dfrac{3}{4} \\ [\mathbf{u}_w + (\delta - 1)\mathbf{u}_f] + \dfrac{1 - \delta}{1 + \delta}[2\mathbf{u}_w + (\delta - 1)\mathbf{u}_{ff}] & \text{if} \quad \delta < \dfrac{3}{4} \end{cases}$$
$$T_b = \begin{cases} \dfrac{1}{\delta}[T_w + (\delta - 1)T_f] & \text{if} \quad \delta \geqslant \dfrac{3}{4} \\ [T_w + (\delta - 1)T_f] + \dfrac{1 - \delta}{1 + \delta}[2T_w + (\delta - 1)T_{ff}] & \text{if} \quad \delta < \dfrac{3}{4} \end{cases} \tag{4.8}$$

where T_f, T_{ff}, $\mathbf{u}_f$ and $\mathbf{u}_{ff}$ are the temperature and velocity in the node x_f and x_{ff}, respectively.

The non-equilibrium distribution function at the boundary nodes $g_{\overline{k}}^{neq}(x_b, t)$ could be approximated by

$$g_k^{neq}(x_b, t) = \begin{cases} g_k^{neq}(x_f, t) & \text{if} \quad \delta \geqslant \dfrac{3}{4} \\ \delta g_k^{neq}(x_f, t) + (1 - \delta)g_k^{neq}(x_{ff}, t) & \text{if} \quad \delta < \dfrac{3}{4} \end{cases} \tag{4.9}$$

In this estimation, the second order approximation of Chapman–Enskog and Taylor series expansions are used, which were presented by Yan and Zu (2008).

5. Results and discussions

In this study, a simulation of natural convection around a horizontal cylinder laid under an insulation wall is carried out using the Lattice Boltzmann Method. The effect of the Rayleigh number in the range of 1000 to 40000 and L/D ratio (the distance from the cylinder to the insulation wall divided by cylinder diameter) ranging from 0.5 to 1.5 is also taken into consideration. The gird sensitivity was tested using three levels of grid size (1120×224, 1400×280 and 1680×336). The results show small differences on the average Nusselt number between the three sets of grid size, so the moderate grid case 1400×280 is selected to simulate the thermal and fluid field. By this selection, the size of D in the lattice unit is equal to 70.

The local Nusselt number is defined as

$$\mathrm{Nu}_L = \frac{-k_c \frac{\partial T}{\partial r}\Big|_{r=\frac{D}{2}} D}{(\Theta_c - \Theta_\infty) k_{fi}} \tag{5.1}$$

where k_c and k_f are the thermal conductivity of air evaluated at the cylinders surface temperature T_c and at the film temperature $\Theta_{fi} = (\Theta_c + \Theta_\infty)/2$, respectively.

Also, the average Nusselt number can be evaluated as

$$\overline{\mathrm{Nu}}_{avg} = \frac{1}{2\pi} \int_0^{2\pi} \mathrm{Nu}_L \, d\theta \tag{5.2}$$

The criterion of convergency is selected as $\max|(T^{n+1} - T^n)/T^n| \leqslant 10^{-6}$. Furthermore, to ensure the convergence of the solution, the velocity and temperature of some points between the cylinder and adiabatic wall are monitored. When these values were fixed, the solution converged.

Figure 3 illustrates the comparison between the numerical and experimental results for L/D ratios of 0.5 and 0.7 in the Rayleigh value of 250000 and for L/D ratios of 1 and 1.5 in the Rayleigh value of 40000.

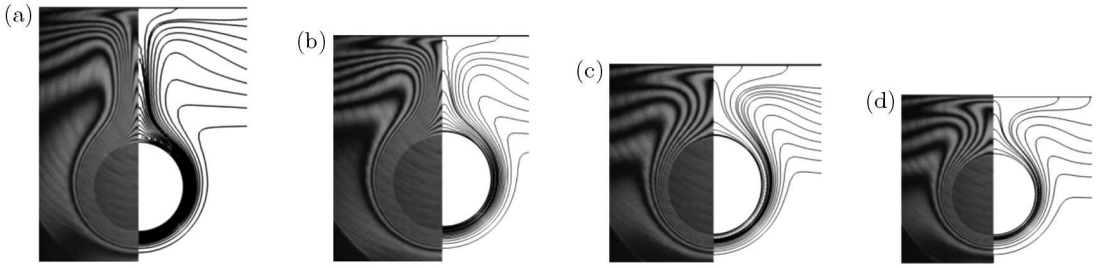

Fig. 3. Isotherms – the right half is the numerical solution and the left half, the experimental results (Ashjaee *et al.*, 2007); (a) $L/D = 1.5$, Ra = 4000, (b) $L/D = 1$, Ra = 4000, (c) $L/D = 0.7$, Ra = 2500, (d) $L/D = 0.5$, Ra = 2500

As can be seen in the figure, the numerical results are in good compatibility with the experimental data obtained by Ashjaee *et al.* (2007).

Streamlines and isotherms for different Rayleigh numbers ranging from 10^4 to 4×10^4 for different values of L/D are shown in Fig. 4.

In general, since there is a temperature gradient between the hot cylinder and the cold fluid, a non-uniform density field is created which results in the development of a buoyant force around the cylinder. Therefore, the fluid ascends the circumference of the cylinder until it reaches the insulation wall located above the cylinder. Then the flow is divided into two similar halves and moves to the left and right directions. As can be seen in Figs. 4(1), with a rise in the Rayleigh number, the flow lines are more concentrated around the cylinder which means

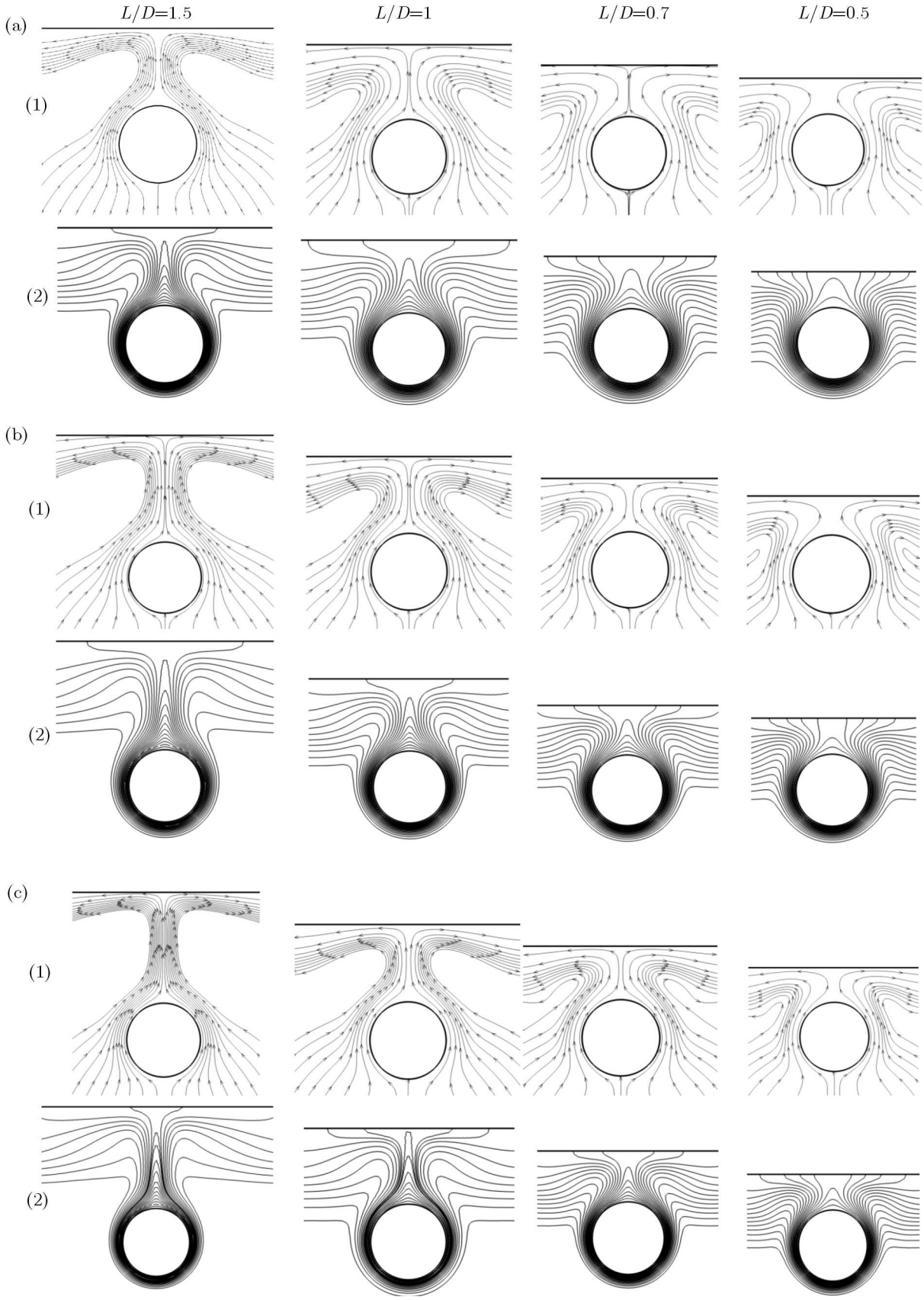

Fig. 4. Distribution diagram (1) flow lines, (2) isothermal lines for different Rayleigh numbers and L/D; (a) $\mathrm{Ra} = 10^4$, (b) $\mathrm{Ra} = 2 \cdot 10^4$, (c) $\mathrm{Ra} = 4 \cdot 10^4$

that the flow intensity has increased and so has the impact of natural convection. According to this phenomenon, it is predicted that with an increase in the Rayleigh number value, the Nusselt number will increase as well. Furthermore, with a fall in the distance from the cylinder to the insulation wall, flow lines interspaces increase. As displayed in Figs. 4(2), the isothermal distribution lines are symmetric. This is due to the fact that the geometry is symmetric around the central axis. In all the cases, a thermal plume is parted from the upper section of the cylinder and moves upward. By increasing the distance from the cylinder to the wall, the thermal plume becomes thinner, sharper and closer to the adiabatic wall. Some of the temperature lines are perpendicular to the adiabatic wall. By moving from 0° to 180°, the concentration of isotherms reduces so the thermal boundary layer has a maximum thickness when approaching to 180 degrees. This process is fully approved by the local Nusselt distribution diagram. As seen in Fig. 5, with a growth in the angle from 0° to 180°, the Nusselt value drops. In this figure, the values of the local Nusselt number obtained by the Lattice Boltzmann Method are compared with the results. The comparison indicates good consistency between the results.

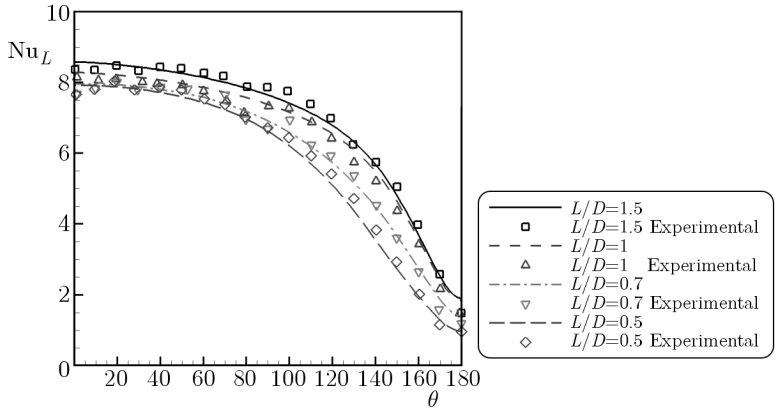

Fig. 5. Local Nusselt distribution around a cylinder and the comparison made with the experimental results (Ashjaee *et al.*, 2007) for different values of L/D when $\mathrm{Ra} = 40000$

Finally, the average Nusselt distribution for different Rayleigh numbers and ratios of L/D is illustrated in Fig. 6. As it is observed, the average Nusselt value shows an upward trend when increasing the Rayleigh number and decreasing the distance from the cylinder to the wall. Moreover, the results present good agreement with the previously obtained experimental results.

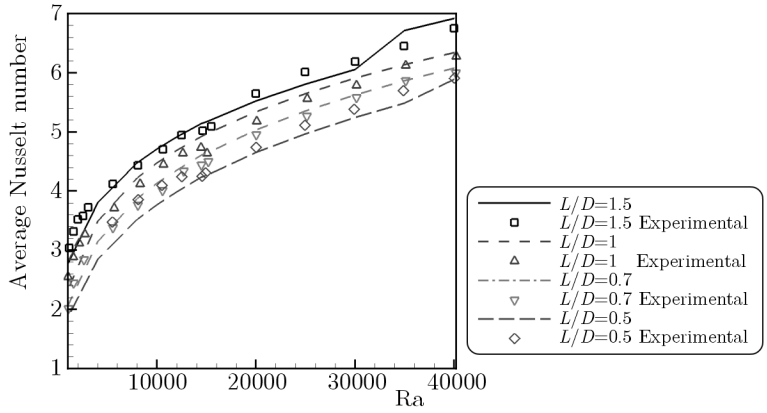

Fig. 6. Average Nusselt distribution based on the Rayleigh number for different ratios of L/D

6. Conclusion

In this paper, numerical solution of natural convective flow around a cylinder laid under an insulation plate has been taken into consideration using the Lattice Boltzmann Method. The impact of variation in the Rayleigh number and the distance from the cylinder to the insulation plate has also been studied.

The results demonstrate that a growth in the angle θ from 0° to 180° leads to a fall in the Nusselt value along the cylinder wall. Also, with an increase in the Rayleigh number and a decrease in the distance ratio, the Nusselt number rises. Furthermore, such great consistency between the numerical solution results and the experimental data represents the strength of the Lattice Boltzmann Method in simulation of natural convection heat transfer in complex geometry.

References

1. Ashjaee M., Eshtiaghi A.H., Yaghoubi M. Yousefi T., 2007, Experimental investigation on free convection from a horizontal cylinder beneath an adiabatic ceiling, *Experimental Thermal and Fluid Science*, **32**, 2, 614-623
2. Bhatnagar P.L, Gross E.P., Krook M., 1954, A model for collision process in gases. I. Small amplitude processes charged and one-component system, *Physical Review A*, **94**, 3, 511-525
3. Dixit H.N., Babu V., 2006, Simulation of high Rayleigh number natural convection in a square cavity using the lattice Boltzmann method, *International Journal of Heat and Mass Transfer*, **49**, 3/4,727-739
4. Fattahi E., Farhadi M., Sedighi K., 2010, Lattice Boltzmann simulation of natural convection heat transfer in eccentric annulus, *International Journal of Thermal Science*, **49**, 12, 2353-2362
5. Filippova O., Hänel D., 1998, Grid refinement for lattice-BGK models, *Journal of Computational Physics*, **147**, 1, 219-228
6. Jami M., Mezrhab A., Bouzidi M., Lallemand P., 2007, Lattice Boltzmann method applied to the laminar natural convection in an enclosure with a heat-generating cylinder conducting body, *International Journal of Thermal Sciences*, **46**, 1, 38-47
7. Jami M., Mezrhab A., Naji H., 2008, Numerical study of natural convection in a square cavity containing a cylinder using the lattice Boltzmann method, *Engineering Computations*, **25**, 5, 480-489
8. Koizumi H., Hosokawa I., 1996, Chaotic behavior and heat transfer performance of natural convection around a hot horizontal cylinder affected by a flat ceiling, *International Journal of Heat and Mass Transfer*, **39**, 5, 1081-1091
9. Ma L., Vander Z., Vander Koo N.F., Nieuwstadt F.T.M., 1994, Natural convection around a horizontal circular cylinder in infinite space and within confining plates: a finite element solution, *Numerical Heat Transfer, Part A*, **25**, 4, 441-456
10. Marsters G.F., 1975, Natural convection heat transfer from a horizontal cylinder in the presence of nearby walls, *The Canadian Journal of Chemical Engineering*, **53**, 1, 144-149
11. Mehrizi A.A., Farhadi M., Afroozi H.H., Sedighi K., Darzi A.A.R., 2012, Mixed convection heat transfer in a ventilated cavity with hot obstacle: effect of nanofluid and outlet port location, *International Communication in Heat and Mass Transfer*, **39**, 7, 100-1008
12. Mehrizi A.A., Farhadi M., Sedighi K., Delavar M.A., 2013, Effect of fin position and porosity on heat transfer improvement in a plate porous media heat exchanger, *Journal of the Taiwan Institute of Chemical Engineers*, **44**, 3, 420-431
13. Mei R., Luo L.S., Shyy W., 1999, An accurate curved boundary treatment in the lattice Boltzmann method, *Journal of Computational Physics*, **155**, 2, 307-330

14. Mohammad A.A., 2007, *Applied Lattice Boltzmann Method for Transport Phenomena Momentum Heat and Mass Transfer*, Calgary, University of Calgary Press

15. Mohammad A.A., El-Ganaoui M., Bennacer R., 2009, Lattice Boltzmann simulation of natural convection in an open ended cavity, *International Journal of Thermal Sciences*, **48**, 10, 1870-1875

16. Mohammad A.A., Kuzmin A., 2010, A critical evaluation of force term in lattice Boltzmann method, natural convection problem, *International Journal of Heat and Mass Transfer*, **53**, 5/6, 990-996

17. Morgan V.T., 1975, The overall convective heat transfer from smooth circular cylinder, *Advances in Heat Transfer*, **11**, 199-264

18. Peng Y., Chew Y.T., Shu C., 2003, Numerical simulation of natural convection in a concentric annulus between a square outer cylinder and a circular inner cylinder using the Taylor-series-expansion and least-squares-based lattice Boltzmann method, *Physical Review E*, **67**, 2, 026701

19. Qureshi Z.H., Ahmad R., 1989, Natural convection from a uniform heat flux horizontal cylinder at moderate Rayleigh numbers, *Numerical Heat Transfer*, **11**, 2, 199-212

20. Sadeghipour M., Razi Y., 2001, Natural convection from a confined horizontal cylinder: the optimum distance between the confining walls, *International Journal of Heat and Mass Transfer*, **44**, 2, 367-374

21. Saitoh T., Sajiki T., Maruhara K., 1993, Bench mark solution to natural convection heat transfer problem around the horizontal circular cylinder, *International Journal of Heat and Mass Transfer*, **36**, 5, 1251-1259

22. Shan X., Chen H., 1993, Lattice Boltzmann model for simulating flows with multiple phases and components, *Physical Review E*, **47**, 3, 1815

23. Yan Y.Y., ZuY.Q., 2008, Numerical simulation of heat transfer and fluid flow past a rotating isothermal cylinder-A LBM approach, *International Journal of Heat Mass Transfer*, **51**, 9/10, 2519-2536

24. Zou Q., He X., 1997, On pressure and velocity boundary conditions for the Lattice Boltzmann BGK model, *Physics of Fluids*, **9**, 6, 1591-1598

Manuscript received June 8, 2012; accepted for print December 19, 2012